Biochemical and Biophysical Research Communications 437 (2013) 292–299

Contents lists available at SciVerse ScienceDirect

Biochemical and Biophysical Research Communications

journal homepage: www.elsevier.com/locate/ybbrc

Interaction of presequence peptides with human translocase of inner membrane of mitochondria Tim23

Yongqiang Zhang, Honghua Deng, Qing Zhao, Shu Jie Li *

School of Physics Science, Department of Biophysics, Nankai University, Tianjin 300071, PR China

ARTICLE INFO

Article history:
Received 13 June 2013
Available online 28 June 2013

Keywords:
Mitochondria
TIM23 complex
Tim23p
Presequence peptides
Interaction

ABSTRACT

The preprotein translocase of the inner membrane of mitochondria (TIM23 complex) is the main entry gate for proteins of the matrix and the inner membrane. Tim23p, the core component of TIM23 complex, forms the import pore across the inner membrane. However, the interaction between presequence peptides and Tim23p remains unclear. Herein, we investigated the interaction of presequence peptides with the intermembrane space domain of Tim23p ($\mathrm{Tim23_{IMS}}$) by fluorescence and micro-Raman spectroscopy. The fluorescence quenching revealed that the interaction between $\mathrm{Tim23_{IMS}}$ and presequence peptides is mainly electrostatic interaction. Micro-Raman spectroscopy and ANS binding experiments showed that presequence peptides induce a more compact conformation of $\mathrm{Tim23_{IMS}}$. GST pull-down experiments and tryptophan fluorescence indicated that there is no interaction between $\mathrm{Tim23_{IMS}}$ and $\mathrm{Tim50_{IMS}}$.

1. Introduction

The vast majority of mitochondrial proteins are synthesized as precursor proteins on cytosolic ribosomes, subsequently imported into mitochondria [1–3]. The TOM40 complex located in the outer mitochondrial membrane functions as a common entry gate for most mitochondrial proteins [4]. After passing through the TOM40 complex, the precursors with an N-terminal cleavable presequence are transported by the TIM23 complex across the inner membrane.

Tim23p is the central component of TIM23 complex. Before translocation through the hydrophilic channel proceeds, the presequences interact with the soluble, N-terminal domain of Tim23p in the intermembrane space [5]. In our previous work, the structural properties of the intermembrane space domain of human Tim23p ($\mathrm{Tim23_{IMS}}$) were characterized and the results showed that the protein has a limited secondary structure and a not-well defined tertiary packing [6]. The intermembrane space domain of Tim50 ($\mathrm{Tim50_{IMS}}$) induces the Tim23 channel to close, while presequences overcome this effect and activate the channel for translocation [7]. Many studies showed that the interaction between presequence peptides and Tim50 is hydrophobic interaction [8–10]. In previous work, by using fluorescence and micro-Raman spectroscopy, we found that the interaction between human $\mathrm{Tim50_{IMS}}$ and presequence peptides is mainly the electrostatic interaction under physiologically relevant conditions [11]. The interaction of Tim50 with presequence peptides has been intensively studied. However, the details of the interaction between Tim23p and presequence peptides are still unclear.

The Human Tim23p is composed of 208 amino acids, in which the N-terminus (1–74 residues) in the IMS is hydrophilic domain, and the C-terminus (75–208 residues) forms hydrophobic domain in the membrane. The IMS domains of Human Tim23p and yeast Tim23p have an amino acid sequence similarity of 29.5%. To fully understand the biological functions of TIM23 complex at molecular basis, detailed information about the interaction between Tim23p and presequence is necessary. In present study, the interaction of human $\mathrm{Tim23_{IMS}}$ with presequence peptides was investigated by fluorescence and micro-Raman spectroscopy, and the presequence peptides were found to interact with $\mathrm{Tim23_{IMS}}$ mainly through electrostatic interaction, which induce a more compact conformation of $\mathrm{Tim23_{IMS}}$.

2. Materials and methods

2.1. Protein expression and purification

The expression and purification of the $\mathrm{Tim23_{IMS}}$ protein were carried out as described in our previous work [6].

2.2. Presequence peptide

pCoxIV (MLATRVFSLVGKRAISTSVCVR) represents the presequence of human cytochrome c oxidase subunit IV [12]. pHsp60 (MLRLPTVFRQMRPVSRVLAPHLTRA) represents the presequence of

---

* Corresponding author. Fax: +86 22 2350 6973.
E-mail address: shujieli@nankai.edu.cn (S.J. Li).

0006-291X/$ - see front matter © 2013 Elsevier Inc. All rights reserved.
http://dx.doi.org/10.1016/j.bbrc.2013.06.070

human heat shock protein 60 [8]. pALDH (MLRAAARFGPRLGRRLL) represents the presequence of human aldehyde dehydrogenase [9]. pSyn (KTRSRTRMVISVGASFVALSLV) represents the peptide with the same amino-acid composition to the pCox IV but with a scrambled sequence. pCoxIV, pHsp60, pALDH and pSyn were synthetized by Ketai Co. (Shanghai, China).

2.3. Fluorescence quenching

Fluorescent quenching experiments were carried out on an Edinburgh fluorescence spectrometer (NIR 301/2). One titration was performed by adding 320 μM pCoxIV to a cuvette containing 2 ml solution of 6.4 μM Tim23$_{IMS}$ at 25 °C and 35 °C. The volume of added pCoxIV never exceeded 5% of the total volume and the mixture was incubated for 5 min after each adding of pCoxIV. The same measurements were repeated with different presequence peptides, such as pALDH, pHsp60 and pSyn. The excitation wavelength was set at 275 nm with a slit width of 3 nm, and the fluorescence emission spectra were scanned from 290 to 450 nm with a slit width of 1 nm. Another titration was performed by adding 1 mM Tim23$_{IMS}$ solution to a cuvette containing 2 ml solution of 10 μM Tim50$_{IMS}$ at 25 °C. The volume of added Tim23$_{IMS}$ never exceeded 5% of the total volume and the mixture was incubated for 5 min after each adding of Tim23$_{IMS}$. A difference between the fluorescence units of the complex in comparison to the theoretical value, calculated from the individual fluorescence units of Tim50$_{IMS}$ and Tim23$_{IMS}$, was used to calculate the binding affinity. The excitation wavelength was set at 295 nm with a slit width of 1 nm, and the fluorescence emission spectra were scanned from 300 to 500 nm with a slit width of 1 nm. All the titrations were performed in buffer containing 10 mM HEPES buffer, pH 7.4, and 0.15 M NaCl. The spectra of samples were corrected by subtracting the corresponding spectra of buffers in the absence of protein.

Fluorescence quenching data were fitted to the static quenching equation. The static quenching equation [13] is:

$$1/(F_0 - F) = 1/F_0 + 1/(K_A F_0[Q]) = 1/F_0 + K_D/(F_0[Q]) \quad (1)$$

where F_0 and F are the fluorescence intensities in the absence and presence of the quencher, respectively. $[Q]$ is the free concentration of the presequence peptide; K_A is the formation constant and K_D is the dissociation constant.

In order to determinate the interaction characteristics between Tim23$_{IMS}$ and the presequence peptide, such as hydrogen bond, Van der Waals force, electrostatic and hydrophobic interactions, we used the Van't Hoff equation and Gibbs free energy equation as follows:

$$\ln K_A = -\Delta H/RT + \Delta S/R \quad (2)$$

$$\ln(K_2/K_1) = (1/T_1 - 1/T_2)\Delta H/R \quad (3)$$

$$\Delta G = \Delta H - T\Delta S = -RT\ln K \quad (4)$$

where ΔH, ΔG and ΔS are enthalpy, free energy and entropy change, respectively.

2.4. Fluorescence resonance energy transfer

Fluorescence resonance energy transfer experiment was performed at 25 °C. The excitation wavelength was set at 275 nm with a slit width of 3 nm, and the fluorescence emission spectra were scanned from 290 to 450 nm with a slit width of 1 nm. The concentration of Tim23$_{IMS}$ was 6.4 μM in 10 mM phosphate buffer (pH 7.4) containing 0.15 M NaCl. According to Föster's non-radiative energy transfer theory [14], the energy transfer effect is related not only to the distance between the acceptor and donor (r), but also to the critical energy transfer distance (R_0), the equations used were:

$$E = 1 - F/F_0 = (R_0)^6/((R_0)^6 + r^6) \quad (5)$$

$$(R_0)^6 = 8.8 \times 10^{-25} K^2 \varphi N^{-4} J \quad (6)$$

$$\varphi_x/\varphi_{st} = (F_x/F_{st})(A_{st}/A_x) \quad (7)$$

$$J = \left(\sum F(\lambda)\varepsilon(\lambda)\lambda^4\Delta\lambda\right)\Big/\left(\sum F(\lambda)\Delta\lambda\right) \quad (8)$$

where R_0 is the critical distance when the transfer efficiency (E) is 50%, K^2 is the spatial orientation factor of the dipole, N is the refractive index of the medium, φ is the fluorescence quantum yield of the donor, A_x is the absorptance of Tim23$_{IMS}$ at 275 nm. The presequence peptides bound with 8-anilino-1-naphthalene-sulfonate (ANS) through covalent linking were prepared as follows. In briefly, ANS-Cl was prepared firstly, as described in previous paper [15]. And then ANS-Cl and presequence peptides were covalently linked with a molar ratio of 1:1 [16]. The presequence peptides bound with ANS were finally loaded onto a PD MiniTrap G-10 column (GE Healthcare). J is the overlap integral of the fluorescence emission spectrum of the donor and the absorption spectrum of the acceptor, $F(\lambda)$ is the fluorescence intensity of Tim23$_{IMS}$ at wavelength λ, and $\varepsilon(\lambda)$ is the molar absorptivity of the acceptor at wavelength λ.

2.5. Micro-Raman spectroscopy

Micro-Raman spectra were recorded in the range of 400–1800 cm^{-1} on a Renishaw Invia Micro-Raman spectrometer (Britain). An exciting wavelength of 785 nm was provided by a laser source of 5.6 mW. The concentration of Tim23$_{IMS}$ was 10 mg ml^{-1}, and the molar ratio of Tim23$_{IMS}$ to presequence peptide was 1:1. The spectra were integrated for 30 times to effectively eliminate the noise.

2.6. ANS binding measurements

ANS can bind nonpolar surfaces of proteins through its anilinonaphthalene group, which results in a significant increase of its fluorescence [17]. ANS binding experiments were performed at an excitation wavelength of 365 nm with 3 nm slit width and scanned from 400 to 600 nm at 20 °C. Tim23$_{IMS}$ was dialyzed in various pH solutions overnight. 20 mM phosphate buffer was used for pH 9.0, 8.0, 7.4, 7.0 and 6.0; and 20 mM citrate buffer was used for pH 5.0 and 4.0. The protein was incubated with presequence peptide at a molar ratio of Tim23$_{IMS}$ to presequence peptide of 1:1. And then the mixture of presequence peptide and Tim23$_{IMS}$ were incubated with ANS solutions for at least 30 min in the dark. The concentrations of Tim23$_{IMS}$ and ANS were 1.6 and 80 μM, giving a molar ratio of ANS to protein of 50. The spectra of samples were corrected by subtracting the corresponding spectra of buffers in the absence of protein.

2.7. GST pull-down experiments

GST pull-down experiments were performed as described in the paper [18]. Briefly, GST-fusion protein (GST-Tim50$_{IMS}$) was purified as described in our previous work [19] and incubated on glutathione Sepharose beads (Amersham Pharmacia) at room temperature for 10 min. Beads were then washed three times with wash buffer (20 mM phosphate buffer, pH 7.4, 0.15 M NaCl). After that, Tim23$_{IMS}$ was added with a molar ratio of Tim23$_{IMS}$ to Tim50$_{IMS}$ of 4:1, and incubation was continued for 30 min at room temperature. The beads were then washed three times in wash buffer, pelleted at 500 g for 30 s and finally analyzed on SDS–PAGE gels.

3. Results

3.1. Interaction of Tim23$_{IMS}$ with presequence peptides is mainly electrostatic interaction

Domain structures of human Tim23p, human Tim23$_{IMS}$, yeast Tim23p, and yeast Tim23$_{IMS}$ were shown in Fig. 1A. As shown in Fig 1B, the similarity of the amino acid sequence of human Tim23$_{IMS}$ with yeast Tim23$_{IMS}$ is 29.5% and there are three tyrosine residues in human Tim23$_{IMS}$.

To estimate the interaction between the presequence peptide and Tim23$_{IMS}$, we performed the fluorescent quenching experiment and used the Eq. (1). As shown in Fig. 2A–D, the dissociation constants (K_D) estimated from the slopes (Table 1) suggested that the binding of presequence peptides with Tim23$_{IMS}$ is strong compared with the binding of pSyn with Tim23$_{IMS}$ and the binding of presequence peptides with Tim23$_{IMS}$ is specific.

We used the Eqs. (2)–(4) to determine the interaction characteristics between Tim23$_{IMS}$ and the presequence peptides. ΔH, ΔS, ΔG obtained from the equations (Table 2) showed that the interaction between Tim23$_{IMS}$ and presequence peptides is mainly electrostatic interaction in 0.15 M NaCl [20]. To further estimate whether there is hydrophobic interaction between Tim23$_{IMS}$ and presequence peptides, we performed the same fluorescent quenching experiments in 1 M NaCl. The results from K_D, ΔH, ΔS, ΔG showed that there is hydrophobic interaction in 1 M NaCl. Therefore, presequence peptides interact with Tim23$_{IMS}$ through both electrostatic interaction and hydrophobic interaction under physiologically relevant conditions, but mainly electrostatic interaction.

3.2. Distance between Tim23$_{IMS}$ and presequence peptide

Electronic excitation energy can be transferred non-radiatively between a fluorescent energy donor and a suitable energy acceptor over distances ranging from 1 to 10 nm. To calculate the distance between Tim23$_{IMS}$ and presequence peptide, we used the Eqs. (5)–(8). The overlap of the absorption spectrum of presequence peptide bound with ANS and the fluorescence emission spectrum of Tim23$_{IMS}$ were shown in Fig. 2E–G, and J values were evaluated by integrating the spectra in Fig. 2E–G for the range of λ from 290 to 450 nm. Under these experimental conditions, we got J, φ_x, R_0, the energy transfer effect (E) and the distance (r) between Tim23$_{IMS}$ and presequence peptides (Table 3) using $K^2 = 2/3$, $N = 1.336$ [21], $\varphi_{st} = 0.14$ [22].

3.3. Tim23$_{IMS}$ forms a more compact conformation with presequence peptide

To obtain more details about the interaction of Tim23p with presequence peptides, we used micro-Raman spectroscopy and ANS binding experiments. The Raman spectra of Tim23$_{IMS}$ and the complex of Tim23$_{IMS}$ with presequence peptide were shown in Fig. 3A, which indicated many conformational details (Table 4). The bands located at 1240–1260 cm^{-1} are useful to detect random coils [23,24]. The band at 1248 cm^{-1} disappeared in line c-e indicated that the random coils of Tim23$_{IMS}$ decreased due to the interaction of Tim23$_{IMS}$ with presequence peptide. As shown in Fig. 3B, the ANS fluorescence spectra of Tim23$_{IMS}$ bound with presequence peptide at a molar ratio of Tim23$_{IMS}$ to presequence peptide of 2:1 and 1:1 (lines 2 and 3), respectively, nearly coincided and a pronounced decrease in ANS fluorescence intensity took place compared with the ANS fluorescence spectrum of Tim23$_{IMS}$ without presequence peptide (line 1). The results indicated that Tim23$_{IMS}$ formed a more compact interior conformation with presequence peptide. These results were consistent with the results measured by micro-Raman spectroscopy. The complex of Tim23$_{IMS}$ and presequence peptide in the presence of 1 M NaCl (Fig. 3C), showed the similar spectral changes as Fig. 3B. However, a complete dissociation were not observed even at the high concentration of salt in Fig. 3C, indicating that hydrophobic force also played an important role in complex formation. These results were consistent with the results measured by fluorescent quenching experiments.

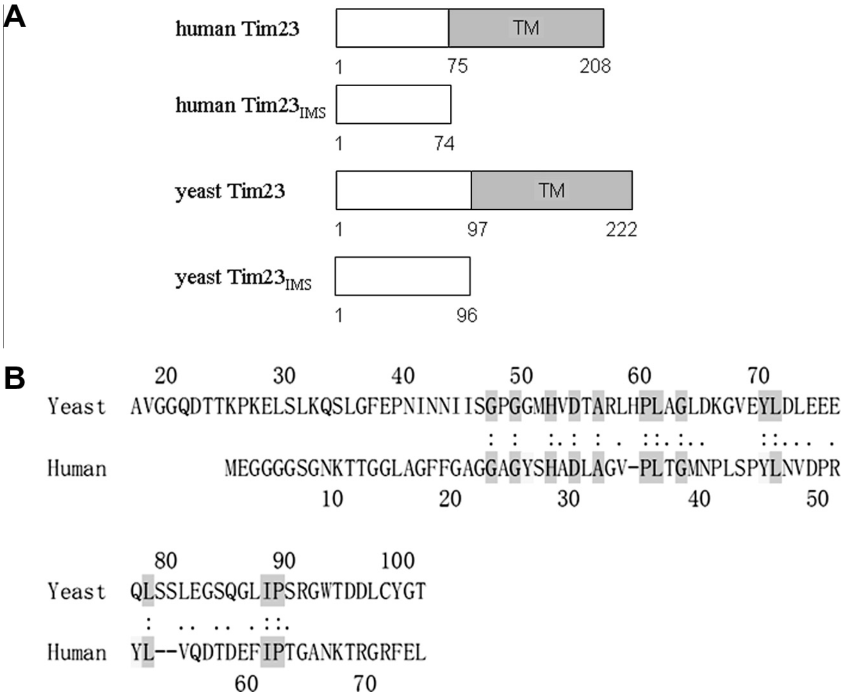

Fig. 1. (A) Domain structures of human Tim23p, human Tim23$_{IMS}$, yeast Tim23p, and yeast Tim23$_{IMS}$ are represented by bar diagrams. The numbers indicate the boundaries of these domains. (B) Amino acid sequence similarity alignments of the human Tim23$_{IMS}$ and yeast Tim23$_{IMS}$ in (A). Human Tim23$_{IMS}$ and yeast Tim23$_{IMS}$ have a similarity of 29.5%.

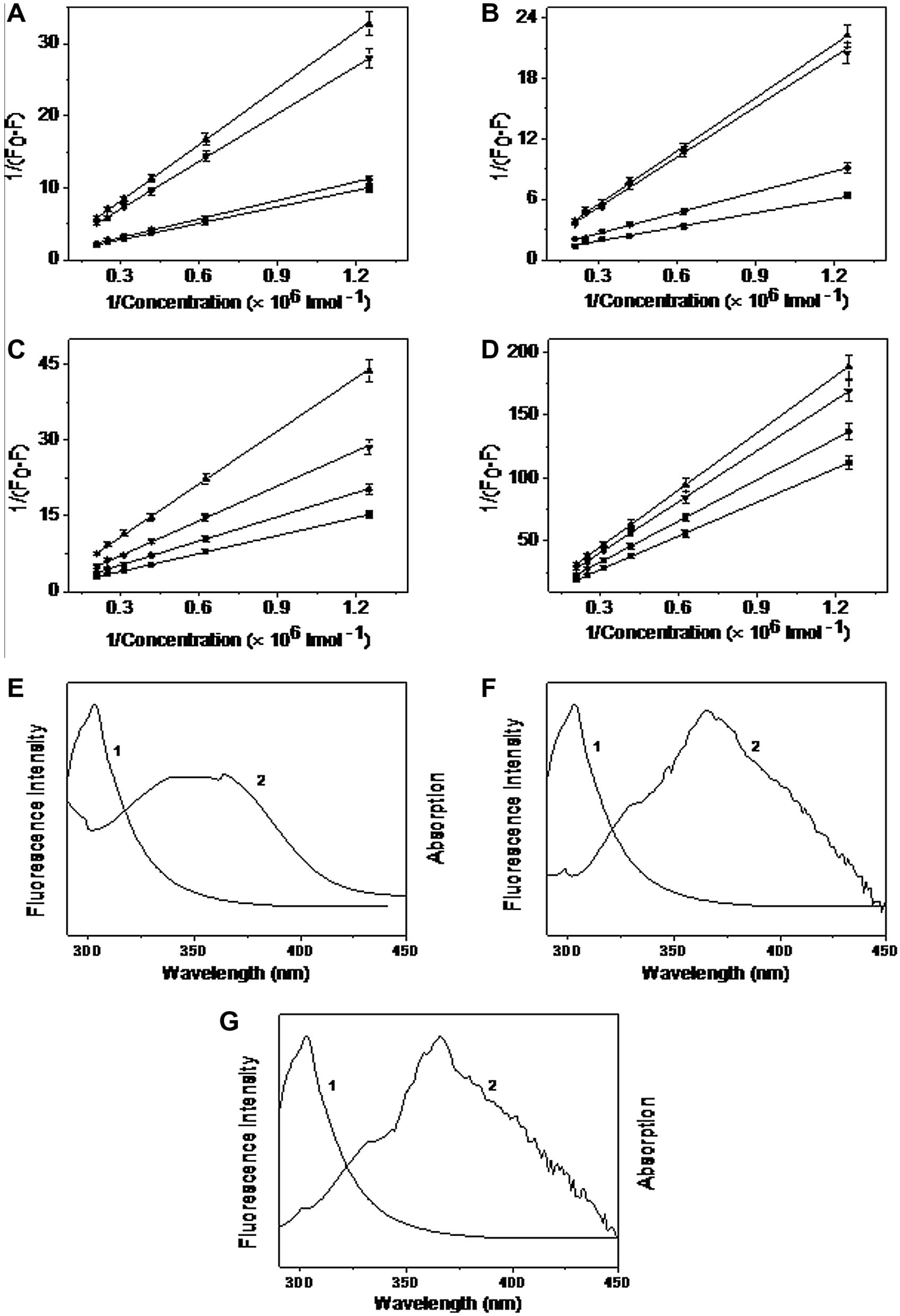

Fig. 2. (A–D) The static quenching plots for the fluorescence quenching of Tim23$_{\mathrm{IMS}}$ by pCoxIV, pALDH, pHsp60 and pSyn, respectively. (E–G) Overlap of the fluorescence emission spectrum of Tim23$_{\mathrm{IMS}}$ with the absorption spectrum of pCoxIV-ANS, pALDH-ANS and pHsp60-ANS, respectively. The concentration of Tim23$_{\mathrm{IMS}}$ was 6.4 μM. The fluorescence emission spectrum of Tim23$_{\mathrm{IMS}}$ was performed at an excitation wavelength of 275 nm. ■, 25 °C, 0.15 M NaCl; ●, 35 °C, 0.15 M NaCl; ▲, 25 °C, 1 M NaCl; ▼, 35 °C, 1 M NaCl. (1) The fluorescence emission spectrum of Tim23$_{\mathrm{IMS}}$. (2) The absorption spectrum of presequence-ANS.

To further test the pH-dependent conformational changes of Tim23$_{\mathrm{IMS}}$ induced by presequence peptide, we analyzed the conformational changes of the complex of Tim23$_{\mathrm{IMS}}$ with presequence peptide at a molar ratio of Tim23$_{\mathrm{IMS}}$ to presequence peptide of 1:1 (Fig. 3D) by ANS binding experiments at various pH. With pH decreasing from 9.0 to 4.0 (lines a–f), a decrease in ANS

Table 1
Dissociation constants of presequence peptides with Tim23$_{\text{IMS}}$ measured by fluorescence quenching.

	K_D (μM)			
	0.15 M NaCl		1.0 M NaCl	
	25 °C	35 °C	25 °C	35 °C
Tim23$_{\text{IMS}}$-pALDH	10.09 ± 0.12	11.78 ± 0.14	58.79 ± 0.59	34.71 ± 0.33
Tim23$_{\text{IMS}}$-pHsp60	28.16 ± 0.34	29.64 ± 0.36	70.50 ± 0.87	56.71 ± 0.69
Tim23$_{\text{IMS}}$-pCox IV	12.98 ± 0.17	14.71 ± 0.21	59.91 ± 0.73	48.75 ± 0.61
Tim23$_{\text{IMS}}$-pSyn	154.19 ± 1.75	181.53 ± 2.31	324.15 ± 4.29	241.27 ± 3.08

Table 2
Thermodynamics of protein-presequence peptide association.

	ΔH (kJ mol^{-1})	ΔS (J K^{-1} mol^{-1})	ΔG (kJ mol^{-1})
10 mM HEPES buffer (pH 7.4), 0.15 M NaCl			
Tim23$_{\text{IMS}}$-pALDH	−11.83	55.92	−28.49
Tim23$_{\text{IMS}}$-pHsp60	−3.90	73.99	−25.95
Tim23$_{\text{IMS}}$-pCox IV	−9.52	61.55	−27.86
10 mM HEPES buffer (pH 7.4), 1.0 M NaCl			
Tim23$_{\text{IMS}}$-pALDH	40.19	215.82	−24.12
Tim23$_{\text{IMS}}$-pHsp60	16.60	135.15	−23.67
Tim23$_{\text{IMS}}$-pCox IV	15.72	133.56	−24.08

Table 3
Distances measured by fluorescence resonance energy transfer.

	Tim23$_{\text{IMS}}$-pALDH	Tim23$_{\text{IMS}}$-pHsp60	Tim23$_{\text{IMS}}$-pCox IV
Efficiency of energy transfer, E	0.0795	0.0527	0.0584
Quantum yield, φ_x	0.3803	0.3803	0.3803
Overlap integral, $J \times 10^{-15}$ (cm^3 M^{-1})	0.456	0.470	1.480
Critical distance, R_0 (nm)	1.7811	1.7901	2.1672
Distance, r (nm)	2.7	2.9	3.4

fluorescence intensity took place, indicating that the complex formed a more compact conformation under acidic conditions (pH 4.0 and pH 5.0).

3.4. No interaction between Tim23$_{\text{IMS}}$ and Tim50$_{\text{IMS}}$

To examine whether Tim23$_{\text{IMS}}$ interacts with Tim50$_{\text{IMS}}$ or not, we performed GST pull-down and fluorescence titration experiments. As shown in Fig. 4A, the band of Tim23$_{\text{IMS}}$ was not observed in lane 3, which showed that there is no interaction between Tim23$_{\text{IMS}}$ and Tim50$_{\text{IMS}}$. The fluorescence titration experiments (Fig. 4B) showed the relative Δ fluorescence intensity (Fig. 4C), indicating no changes of the fluorescence of Tim50$_{\text{IMS}}$ with and without Tim23$_{\text{IMS}}$. It also showed that there is no interaction between Tim23$_{\text{IMS}}$ and Tim50$_{\text{IMS}}$.

4. Discussion

Tim23p is the central component of the TIM23 complex, in which it performs a number of functions. Before translocation proceeds, precursor proteins are recognized by Tim23$_{\text{IMS}}$ [5]. Though the interaction of Tim23p with presequence peptides has been intensively studied, the details are still unknown. The fluorescence spectroscopy has been widely used to study protein conformational transitions, subunit association, substrate binding, or denaturation [25,26], but it is rarely reported to be used in the investigation on the interaction of proteins with peptides. In present study, we used fluorescence quenching and fluorescence resonance energy transfer to study the interaction between Tim23$_{\text{IMS}}$ and presequence peptides. The results showed that presequence peptides interact with Tim23$_{\text{IMS}}$ through both electrostatic interaction and hydrophobic interaction under physiologically relevant conditions, but mainly electrostatic interaction. Though the Micro-Raman spectroscopy has been used to study conformational changes of proteins, the interaction of proteins with peptides studied by this method has been rarely reported. In our manuscript, we have investigated the interaction of Tim23$_{\text{IMS}}$ with presequence peptides by this method, and showed that Tim23$_{\text{IMS}}$ forms a more compact conformation with the presequence peptide.

It was reported that Tim23$_{\text{IMS}}$ might function as hub in the mitochondrial import machinery protein network, and a distinct binding region of yeast Tim23$_{\text{IMS}}$ formed by residues 71–84 was found to be important by using NMR spectroscopy [27]. In our previous work, we characterized the structural properties of human Tim23$_{\text{IMS}}$ and showed that the protein has a limited secondary structure and a not-well defined tertiary packing [6]. In this case, we found that Tim23$_{\text{IMS}}$ forms a more compact conformation with the presequence peptide.

It is known that Tim50$_{\text{IMS}}$ induces the Tim23 channel to close, while presequences overcome this effect and activate the channel for translocation [7]. Many studies showed that the interaction between presequence peptides and Tim50 is hydrophobic interaction [8–10]. In our previous work, we purified human Tim50$_{\text{IMS}}$ [19] and studied the interaction between Tim50$_{\text{IMS}}$ and presequence peptides by using micro-Raman and fluorescence spectroscopy [11]. The results showed that there are both electrostatic interaction and hydrophobic interaction between human Tim50$_{\text{IMS}}$ and presequence peptides, and the interaction is mainly electrostatic interaction under physiologically relevant conditions. Qian et al. [28] reported that Tim50 contains a large groove as putative binding site for presequences and the groove contains several exposed negatively charged residues, which may be ideally suited as a binding site for positively charged presequences/preproteins. Many previous studies showed that the electrostatic interaction may be important for the import of the precursor proteins. In present work, we found that there are both electrostatic interaction and hydrophobic interaction between human Tim23$_{\text{IMS}}$ and presequence peptides, and the interaction is mainly through electrostatic interaction under physiologically relevant conditions. These results of human Tim23$_{\text{IMS}}$ agree with the ones of human Tim50$_{\text{IMS}}$, and it showed that the electrostatic interaction should be important for the import of the precursor proteins.

Fluorescence resonance energy transfer has been widely used to study protein interaction. In our case, the excitation wavelength was set at 275 nm which excites the fluorescence of tyrosine. Therefore, the distances between a fluorescent energy donor tyrosine and an energy acceptor ANS estimated from fluorescence resonance energy transfer indicated the distances between presequence peptides and Tim23$_{\text{IMS}}$, which indirectly revealed the interaction between presequence peptides and Tim23$_{\text{IMS}}$. As shown in Fig. 1B, the similarity of the amino acid sequence of human Tim23$_{\text{IMS}}$ with yeast Tim23$_{\text{IMS}}$ is 29.5% and there are three tyrosine residues in human Tim23$_{\text{IMS}}$. It was reported that a

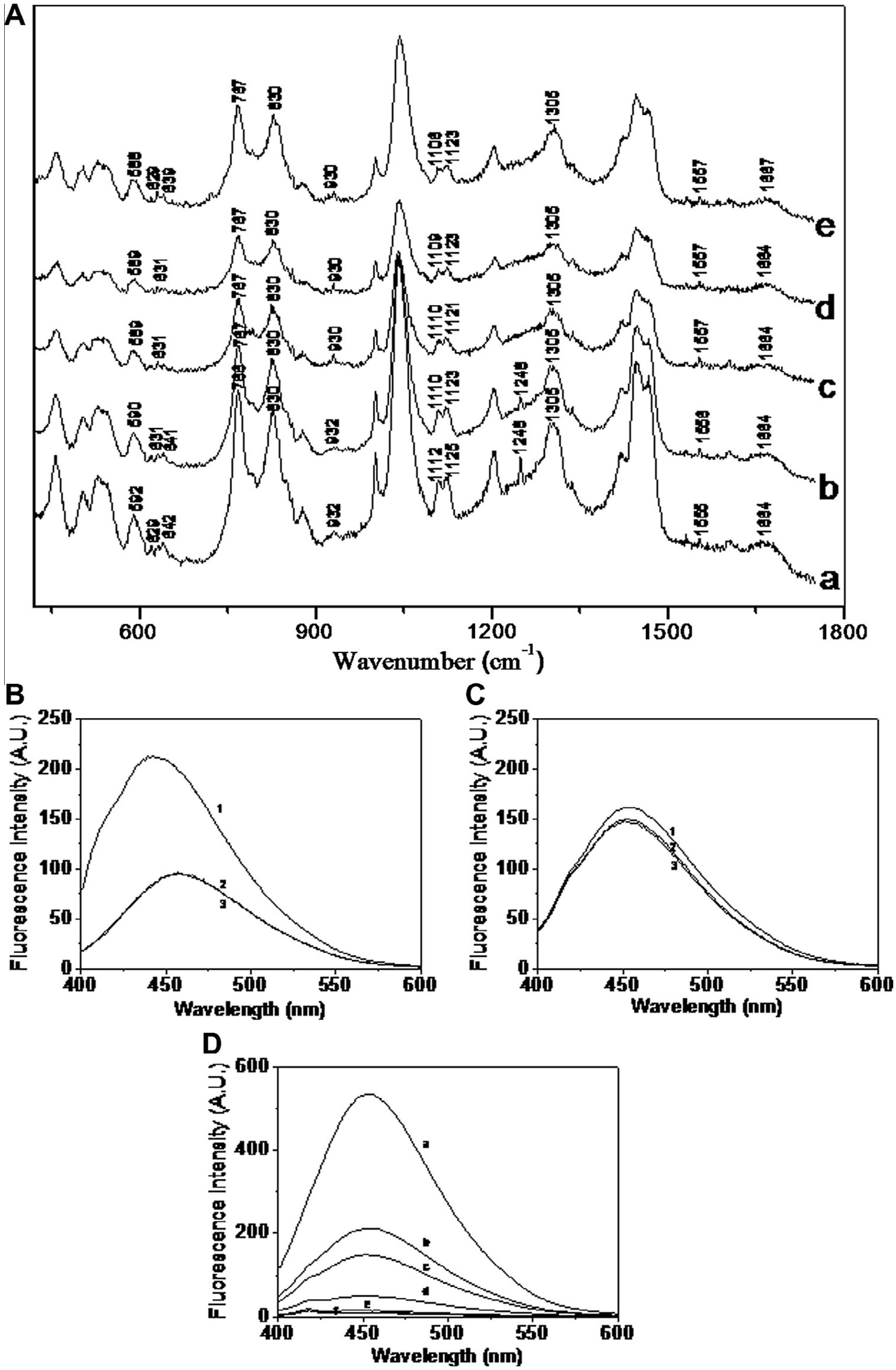

Fig. 3. (A) Micro-Raman spectrum of Tim23$_{IMS}$ and the complex of Tim23$_{IMS}$ with presequence peptides. The micro-Raman spectroscopy was performed at 20 °C with an excitation wavelength of 785 nm in the range of 400–1800 cm^{-1}. The molar ratio of Tim23$_{IMS}$ to presequence peptide was 1:1 and the concentration of Tim23$_{IMS}$ was 10 mg/ml. a, Tim23$_{IMS}$; b, Tim23$_{IMS}$ + pSyn; c, Tim23$_{IMS}$ + pALDH; d, Tim23$_{IMS}$ + pCoxIV; e, Tim23$_{IMS}$ + pHsp60. (B) Effect of varying molar ratio of Tim23$_{IMS}$ to presequence peptide on ANS fluorescence in 20 mM phosphate buffer (pH 7.4) containing 0.15 M NaCl at 20 °C. (C) Effect of varying molar ratio of Tim23$_{IMS}$ to presequence peptide on ANS fluorescence in 20 mM phosphate buffer (pH 7.4) containing 1 M NaCl at 20 °C. 1, Tim23$_{IMS}$: presequence = 1:0; 2, Tim23$_{IMS}$: presequence = 1:0.5; 3, Tim23$_{IMS}$: presequence = 1:1. The concentration of Tim23$_{IMS}$ was 1.6 μM. (D) Effect of varying pH of the complex of Tim23$_{IMS}$ with presequence peptide on ANS fluorescence. Tim23$_{IMS}$ was dialyzed in various pH solutions overnight. 20 mM phosphate buffer was used for pH 9, 8, 7 and 6; and 20 mM citrate buffer was used for pH 5 and 4. The concentration of Tim23$_{IMS}$ was 1.6 μM. The molar ratio of Tim23$_{IMS}$ to presequence peptide was 1:1. a, pH 9; b, pH 8; c, pH 7; d, pH 6; e, pH 5; f, pH 4.

distinct binding region of yeast Tim23$_{IMS}$ formed by residues 71–84 is important, and the residue Leu-71 was found to be the largest chemical shift change by using NMR spectroscopy [27]. Compared with the amino acid sequence of yeast Tim23$_{IMS}$, the residue Tyr-45 in human Tim23$_{IMS}$ was similar to the residue Tyr-70 in yeast Tim23$_{IMS}$ which can be easily influenced by the residue Leu-71. So we speculated that the interaction between human Tim23$_{IMS}$ and presequence peptides may influence the residue Tyr-45.

Table 4
Assignment of the main bands in the Raman spectra of $\text{Tim23}_{\text{IMS}}$.

Assignments	Raman wavenumbers of $\text{Tim23}_{\text{IMS}}$ (cm^{-1})	Raman wavenumbers of $\text{Tim23}_{\text{IMS}}$ with pSyn (cm^{-1})	Raman wavenumbers of $\text{Tim23}_{\text{IMS}}$ with pALDH (cm^{-1})	Raman wavenumbers of $\text{Tim23}_{\text{IMS}}$ with pCox IV (cm^{-1})	Raman wavenumbers of $\text{Tim23}_{\text{IMS}}$ with pHsp60 (cm^{-1})
α-Helix	932	932	930	930	930
β-Sheet	1305	1305	1305	1305	1305
Random coil	1248, 1664	1248, 1664	1664	1664	1667
C–N	1112, 1125	1110, 1123	1110, 1121	1109, 1123	1106, 1123
Tyrosine	830	830	830	830	830
Amide I[a]	1664	1664	1664	1664	1667
Amide II[b]	1555	1556	1557	1557	1557
Amide III[c]	1248, 1305	1248, 1305	1305	1305	1305
Amide IV[d]	629, 642, 766	631, 641, 767	631, 767	631, 767	629, 639, 767
Amide V[e]	642,766	641,767	767	767	767
Amide VI[f]	592	590	589	589	588

[a] Amide I: C=O stretching, N–H deformation vibration, C–N stretching.
[b] Amide II: C–N stretching, N–H deformation vibration.
[c] Amide III: C–N stretching, N–H deformation vibration.
[d] Amide IV: O=C–N deformation vibration.
[e] Amide V: N–H deformation vibration.
[f] Amide VI: C=O deformation vibration.

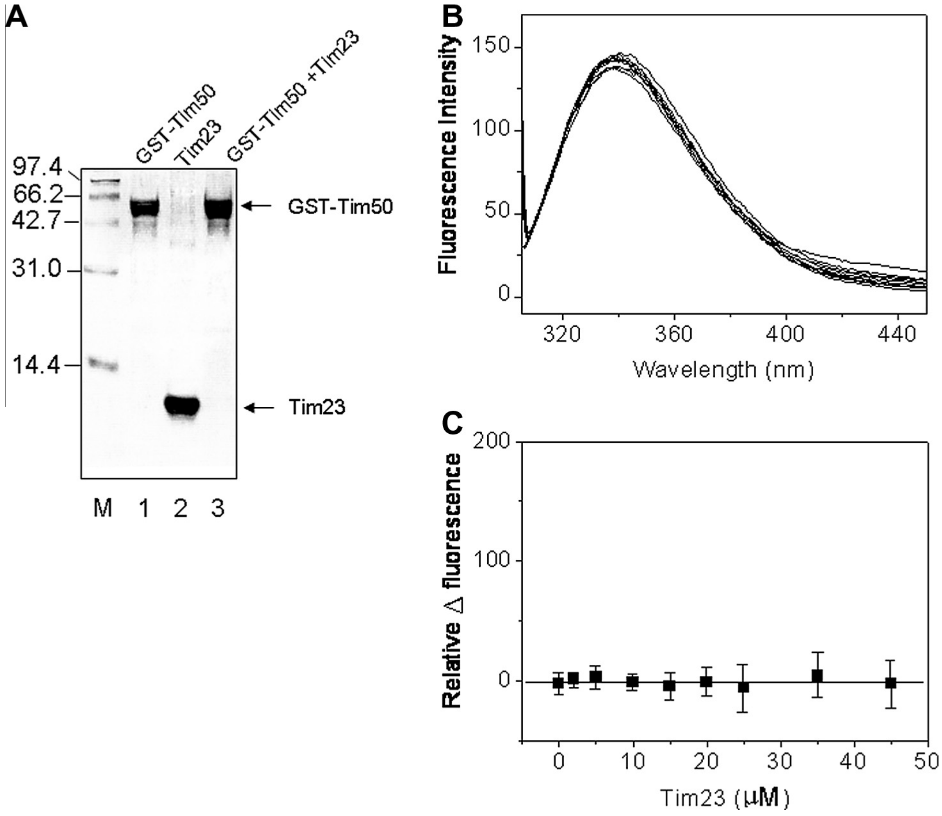

Fig. 4. (A) SDS–PAGE for the interaction between $\text{Tim23}_{\text{IMS}}$ and $\text{Tim50}_{\text{IMS}}$ in a GST pull-down assay. M, molecular weight markers; lane 1, GST-$\text{Tim50}_{\text{IMS}}$; lane 2, $\text{Tim23}_{\text{IMS}}$; lane 3, $\text{Tim23}_{\text{IMS}}$ incubated with GST-$\text{Tim50}_{\text{IMS}}$ on glutathione Sepharose beads at room temperature. The beads were then washed three times in wash buffer, pelleted at 500 g for 30 s and finally analyzed on SDS–PAGE gels. Numbers to the left of the panel indicate the migrations of molecular weight markers (in kDa). (B) Fluorescence spectra of $\text{Tim50}_{\text{IMS}}$ titrated by $\text{Tim23}_{\text{IMS}}$. (C) Binding of $\text{Tim23}_{\text{IMS}}$ to $\text{Tim50}_{\text{IMS}}$ measured by fluorescence spectroscopy. Data points represent a difference between the fluorescence units of the complex in comparison to the theoretical value, calculated from the individual fluorescence units of $\text{Tim50}_{\text{IMS}}$ and $\text{Tim23}_{\text{IMS}}$, and the bars represent standard errors.

For the translocation of the N-terminal presequence across the inner membrane, mitochondrial membrane potential ($\Delta\varphi$) is required [29]. Proton pumps in mitochondrial inner membrane pump protons into intermembrane space and keep the inner membrane potential ($\Delta\varphi$) and the pH gradient between matrix and intermembrane space. Therefore, the pH in intermembrane space would affect the function and conformation of Tim23p. Our work revealed that $\text{Tim23}_{\text{IMS}}$ formed a more compact conformation with presequence peptide under acidic conditions (pH 4.0 and pH 5.0).

$\text{Tim23}_{\text{IMS}}$ is in a molten globular state in solution, which might be interpreted in two ways. One possibility is that the protein interacts with preproteins, which may be responsible for the protein structural stability [30]. Another possibility is that the lack of $\text{Tim50}_{\text{IMS}}$ that interacts with the Tim23p [31]. Marom et al. [8]

used the cross-linking to detect the complex formation, and there is no cross-linking products of the $Tim23_{IMS}$–$Tim50_{IMS}$ complex in lane 3 (from left to right) of Fig. 4. In our work, we found that the random coil of human $Tim23_{IMS}$ decreased when it interacted with the presequence peptide and there is no interaction between human $Tim23_{IMS}$ and $Tim50_{IMS}$, suggesting that Tim23p interacts with preproteins, which may be responsible for the protein structural stability.

Acknowledgments

This work was supported by National Natural Science Foundation of China (Nos. 30970579 and 31271464), and the Ph.D. Programs Foundation of Ministry of Education of China (Nos. 20110031110004 and 20120031110028).

References

[1] K. Gabriel, T. Lithgow, S.K. Buchanan, The alpha and the beta: protein translocation across mitochondrial and plastid outer membranes, Trends. Biochem. Sci. 26 (2001) 36–40.

[2] N. Pfanner, N. Wiedemann, C. Meisinger, et al., Assembling the mitochondrial outer membrane, Nat. Struct. Mol. Biol. 11 (2004) 1044–1048.

[3] M.T. Ryan, R. Wagner, N. Pfanner, The transport machinery for the import of preproteins across the outer mitochondrial membrane, Int. J. Biochem. Cell Biol. 32 (2000) 13–21.

[4] T. Endo, K. Yamano, Transport of proteins across or into the mitochondrial outer membrane, Biochim. Biophys. Acta 2010 (1803) 706–714.

[5] M. Van der Laan, D.P. Hutu, P. Rehling, On the mechanism of preprotein import by the mitochondrial presequence translocase, Biochim. Biophys. Acta 2010 (1803) 732–739.

[6] Y. Zhang, Y. Xu, Q. Zhao, et al., The structural characteristics of human preprotein translocase of the inner mitochondrial membrane Tim23: implications for its physiological activities, Protein. Expr. Purif. 82 (2012) 255–262.

[7] M. Meinecke, R. Wagner, P. Kovermann, et al., Tim50 maintains the permeability barrier of the mitochondrial inner membrane, Science 312 (2006) 1523–1526.

[8] M. Marom, D. Dayan, K. Demishtein-Zohary, et al., Direct interaction of mitochondrial targeting presequences with purified components of the TIM23 protein complex, J. Biol. Chem. 286 (2011) 43809–43815.

[9] C. Schulz, O. Lytovchenko, J. Melin, et al., Tim50's presequence receptor domain is essential for signal driven transport across the TIM23 complex, J. Cell. Biol. 195 (2011) 643–656.

[10] H. Yamamoto, N. Itoh, S. Kawano, et al., Dual role of the receptor Tom20 in specificity and efficiency of protein import into mitochondria, Proc. Natl. Acad. Sci. 108 (2011) 91–96.

[11] Y. Zhang, H. Deng, Q. Zhao, et al., Interaction of presequence with human translocase of the inner membrane of mitochondria Tim50, J. Phys. Chem. B 116 (2012) 2990–2998.

[12] K.N. Truscott, P. Kovermann, A. Geissler, et al., A presequence- and voltage-sensitive channel of the mitochondrial preprotein translocase formed by Tim23, Nat. Struct. Biol. 8 (2001) 1074–1082.

[13] Y. Zhang, H. Deng, X. Zhang, et al., Interaction of divalent metal ions with human translocase of inner membrane of mitochondria Tim50, Biochem. Biophys. Res. Commun. 428 (2012) 365–370.

[14] L.A. Sklar, B.S. Hudson, R.D. Simoni, Conjugated polyene fatty acids as fluorescent probes: binding to bovine serum albumin, Biochemistry 16 (1977) 5100–5108.

[15] K. Muramoto, H. Kamiya, Preparation and characterization of photoactivable heterobifunctional fluorescent reagents, Agr. Biol. Chem. 48 (1984) 2695–2699.

[16] W.R. Gray, Methods in Enzymology, Academic Press Inc., New York, 1967.

[17] L. Stryer, The interaction of a naphthalene dye with apomyoglobin and apohemoglobin. A fluorescent probe of non-polar binding sites, J. Mol. Biol. 13 (1965) 482–495.

[18] J. Sambrook, D.W. Russell, Molecular Cloning: A Laboratory Manual, Cold Spring Harbor Lab Press, New York, 2001.

[19] Y. Zhang, Y. Xu, Q. Zhao, et al., Expression and structural characterization of human translocase of inner membrane of mitochondria Tim50, Protein. Expr. Purif. 80 (2011) 130–137.

[20] P.D. Ross, S. Subramanian, Thermodynamics of protein association reactions: forces contributing to stability, Biochemistry 20 (1981) 3096–3102.

[21] L. Cyril, J.K. Earl, W.M. Sperry, Biochemists Handbook, E&F.N. Spon, London, 1961.

[22] F.C. Raymond, Fluorescence quantum yields of tryptophan and tyrosine, Anal. Lett. 1 (1967) 35–42.

[23] J. Bandekar, S. Krimm, Vibrational analysis of peptides, polypeptides, and proteins. VI. Assignment of beta-turn modes in insulin and other proteins, Biopolymers 19 (1980) 31–36.

[24] P.R. Carey, Biochemical Applications of Raman and Resonance Raman Spectroscopies. A Subsidiary of Harcourt Brace Jovanovich, Academic Press, New York, 1982.

[25] M.R. Eftink, The use of fluorescence methods to monitor unfolding transitions in proteins, Biophys. J. 66 (1994) 482–501.

[26] B.E. Jones, J.M. Beechem, C.R. Matthews, Local and global dynamics during the folding of Escherichia coli dihydrofolate reductase by time-resolved fluorescence spectroscopy, Biochemistry 34 (1995) 1867–1877.

[27] L. de la Cruz, R. Bajaj, S. Becker, et al., The intermembrane space domain of Tim23 is intrinsically disordered with a distinct binding region for presequences, Protein Sci. 19 (2010) 2045–2054.

[28] X. Qian, M. Gebert, J. Hopker, et al., Structural basis for the function of Tim50 in the mitochondrial presequence translocase, J. Mol. Biol. 411 (2011) 513–519.

[29] L. Gevorkyan-Airapetov, K. Zohary, D. Popov-Celeketic, et al., Interaction of Tim23 with Tim50 Is essential for protein translocation by the mitochondrial TIM23 complex, J. Biol. Chem. 284 (2009) 4865–4872.

[30] M.F. Bauer, C. Sirrenberg, W. Neupert, et al., Role of Tim23 as voltage sensor and presequence receptor in protein import into mitochondria, Cell 87 (1996) 33–41.

[31] D. Mokranjac, S.A. Paschen, C. Kozany, et al., Tim50, a novel component of the TIM23 preprotein translocase of mitochondria, EMBO J. 22 (2003) 816–825.